Tellus (2006), 58B, 427–437

TELLUS

Using atmospheric CO_2 data to assess a simplified carbon-climate simulation for the 20th century

By RACHEL M. LAW*, EVA A. KOWALCZYK and YING-PING WANG, *CSIRO Marine and Atmospheric Research, PMB 1, Aspendale, Vic 3195, Australia*

(Manuscript received 12 January 2006; in final form 15 May 2006)

ABSTRACT

The CSIRO biosphere model has been coupled to an atmosphere model and a simulation has been performed for the 20th century. Both biosphere and atmosphere are forced with global CO_2 concentration and the atmosphere is also forced with prescribed sea surface temperatures. The simulation follows the C4MIP Phase 1 protocol. We assess the model simulation using atmospheric CO_2 data. Mauna Loa growth rate is well simulated from 1980 but overestimated before that time. The interannual variations in growth rate are reasonably reproduced. Seasonal cycles are underestimated in northern mid-latitudes and are out of phase in the southern hemisphere. The north–south gradient of annual mean CO_2 is substantially overestimated due to a northern hemisphere net biosphere source and a southern tropical sink. Diurnal cycles at three northern hemisphere locations are larger than observed in many months, most likely due to larger respiration than observed.

1. Introduction

Roughly half of the anthropogenic carbon added to the atmosphere over recent decades has been taken up by the biosphere and the ocean. However, we do not know if these reservoirs can continue to absorb carbon at their current rates, particularly as climate changes due to increasing greenhouse gases. To address these questions, coupled climate-carbon simulations have been performed for the past and coming centuries (e.g. Cox et al., 2000; Friedlingstein et al., 2001; Dufresne et al., 2002; Zeng et al., 2004; Matthews et al., 2005). The results indicate a positive feedback, i.e. carbon sinks are reduced under climate change and CO_2 concentrations increase more rapidly than they would otherwise. The magnitude of the feedback remains uncertain with a recent suite of models giving CO_2 enhancement under climate change of 20–200 ppm (Friedlingstein et al., 2006). Reducing this range is an important research task. One contribution to this task is to analyse the coupled simulations for the current century to assess how well the component models perform against any available observations.

Here, we focus on the interaction of the biosphere and the atmosphere and use atmospheric CO_2 measurements to assess the quality of the simulation. Atmospheric measurements respond to surface fluxes from a region and so provide a means to evaluate regional fluxes that may be more reliable than comparing with flux measurements directly. A number of studies (e.g. Heimann et al., 1998; Nemry et al., 1999) have taken this approach and used the seasonal cycle of atmospheric CO_2. More recently Dargaville et al. (2002) have also examined trends in the amplitude of CO_2 and interannual variations. They took the fluxes from four terrestrial models and used an atmospheric transport model to make comparisons with atmospheric CO_2 at 15 locations. They found that the amplitude of the seasonal cycle was generally underestimated compared to observations but that the trend in amplitude from 1980 – 1991 was reasonably reproduced. They also found that the magnitude of interannual variations in atmospheric CO_2 was underestimated. Here, we further extend the comparison with atmospheric CO_2 by also considering the annual mean distribution of atmospheric CO_2 and diurnal variations.

2. Model simulation

We have performed a simplified form of a coupled carbon-climate simulation following the protocol for C4MIP phase 1 (http://www.c4mip.cnrs-gif.fr/protocol.html). This experiment was designed to test the biospheric component of coupled climate-carbon simulations under relatively controlled conditions, to allow easier diagnosis of any problematic behaviour. The experiment has also been performed by Jones and Warnier (2004) using the Hadley Centre model. An overview of the simulation will be followed by details of the prescribed inputs. The atmosphere and biosphere models will be described in Section 3.

*Corresponding author.
e-mail: rachel.law@csiro.au
DOI: 10.1111/j.1600-0889.2006.00198.x

The CSIRO Conformal-cubic Atmospheric Model (CCAM), is run from 1900 – 1999 with prescribed sea surface temperatures (SSTs). The time history of global mean CO_2 is also prescribed for use by the radiation scheme. Using these two forcings ensures that the model produces a reasonable simulation of 20th century climate. The CSIRO Atmosphere Biosphere Land Exchange model (CABLE) is coupled to the atmosphere model to simulate the exchange of CO_2 between the biosphere and atmosphere. The biosphere model is forced with the same global mean CO_2 concentration as used by the radiation scheme. This means that the biosphere will respond to increasing CO_2 and changes in climate but no feedback is allowed on the forcing CO_2. However, atmospheric CO_2 is modelled as a passive tracer. To allow comparison between modelled and observed CO_2, it is also necessary to simulate the other carbon exchanges with the atmosphere. The fluxes, described below, are prescribed and included in the simulation from 1960. The C4MIP phase 1 protocol required the biosphere model to have the ability to simulate CO_2 fluxes due to land-use change. CABLE does not have this ability at present and we used prescribed fluxes instead.

2.1. *SST and CO_2 forcing*

The sea surface temperatures (SSTs) were taken from the HadISST1.1 dataset (Rayner et al., 2003) at $1 \times 1°$ and monthly resolution. The data were interpolated to the CCAM model grid. Within the model, the SSTs are linearly interpolated in time between the monthly data. Global mean SST increases by about 0.6°C over the 20th century with periods of more rapid increase in the 1930s and 1940s and in the 1980s and 1990s. Modelled global mean surface air temperature over land gridpoints shows a similar increase to the SSTs but with more rapid warming in the 1990s. Interannual variations are approximately 0.2 – 0.4°C with larger variations in the land air temperature than in the SSTs.

The global CO_2 forcing is a spline fit to the Law Dome ice core records (Etheridge et al., 1996) prior to 1958 and atmospheric measurements at South Pole and Mauna Loa, Hawaii, after 1958 (Keeling and Whorf, 2005). The CO_2 increases slowly through the first half of the century and then more rapidly. Interannual variations are smoothed from the record but decadal variations remain.

2.2. *CO_2 fluxes*

The ocean CO_2 fluxes are the median fluxes from 11 seasonal models that participated in OCMIP2 (http://www.ipsl.jussieu.fr/OCMIP/phase2/simulations/Abiotic/HOWTO-Abiotic.html). The ocean carbon models were run from 1765–2000 with prescribed atmospheric CO_2. Monthly fluxes from 1850–2000 were provided at $2 \times 2°$ resolution and interpolated to the CCAM grid. Ocean uptake increases from about −1.0 to −2.5 GtC yr^{-1} over the four decades from 1960 when the prescribed fluxes are included in the simulation.

Fossil CO_2 emissions were taken from Andres et al. (1996) with global totals increasing from around 2.5 to 6.5 GtC yr^{-1} from 1960 to 2000. Annual emission patterns were provided for each year from 1900 to 1990 at $3.75 \times 2.5°$ resolution. These were mapped onto the CCAM grid and any fossil emissions in ocean grid-cells were discarded. The lost emissions were accounted for by rescaling all remaining emissions to maintain the global total flux. From 1990 to 1999, the flux distribution was kept constant and global total fluxes were taken from the 2003 version of Marland et al. (2005).

Since CABLE is currently unable to simulate CO_2 fluxes due to land-use change, these fluxes were prescribed using output from other terrestrial models (McGuire et al., 2001). Four models were run from 1860 – 1992 with and without cropland establishment and abandonment. We use the difference in flux between these two simulations to isolate the contribution from land-use change and take the average flux across three of the four models (insufficient data were available for the fourth model). Since the simulations ended in 1992, we kept the fluxes at the 1992 values for 1993–1999. The fluxes range from 0.5 to 1.4 GtC yr^{-1} with a general decrease over the four decades from 1960. The fluxes have no seasonal variation. It is important to note that these fluxes do not include contributions from natural fires and other non-agricultural disturbances. They also do not include forest conversion to pasture and hence are smaller in magnitude through the 1980s and 1990s than the estimates of Houghton (2003).

Each set of fluxes is input to the surface layer of the atmospheric model and each is run as a separate tracer within the model. This allows the contribution from each flux to be assessed separately, although in most cases the analysis is performed on the sum of the four tracers (biosphere, ocean, fossil and land-use). In addition to the fluxes required for the C4MIP protocol, we also ran an extra tracer using the CASA neutral biosphere fluxes (Randerson et al., 1997) as input. These fluxes were used in the TransCom model intercomparison (Gurney et al., 2003) and provide a good baseline with which to compare the fluxes produced by CABLE.

2.3. *Model output*

A wide range of meteorological and carbon variables are output from the model at monthly resolution for the whole atmosphere. In addition, hourly timeseries of a subset of these variables were output for 84 locations where atmospheric CO_2 is sampled and for 39 flux tower locations. The atmospheric CO_2 locations were selected from the GLOBALVIEW (2003) data compilation focussing on sites with longer records. The flux tower locations were selected from the FLUXNET site list (http://www.fluxnet.ornl.gov/fluxnet/siteloc.cfm) focussing on towers with gap-filled data and covering a range of biomes.

3. Model description

3.1. Atmosphere model

CCAM is a global model formulated upon a quasi-uniform grid derived by projecting the panels of a cube onto the surface of the Earth. CCAM is a two time-level semi-implicit hydrostatic primitive equation model as described by McGregor (1987) and McGregor and Dix (2001). Distinctive features of the CCAM dynamics include semi-Lagrangian horizontal advection with bi-cubic spatial interpolation (McGregor, 1993, 1996), total-variation-diminishing vertical advection and an unstaggered grid. CCAM has an extensive set of physical parametrizations: GFDL parametrization for longwave and shortwave radiation, interactive diagnosed cloud distribution, cumulus convection, Tiedke shallow convection, gravity wave drag, diurnally-varying skin temperature for SSTs and evaporation of rainfall.

3.2. Land surface and biosphere model

CABLE is a model of biosphere–atmosphere exchange which includes the aerodynamic and radiative interaction of a canopy with soil and snow underneath and the treatment of canopy turbulence. CABLE is a one layer two-leaf canopy model as described in Wang and Leuning (1998) and it was formulated on the basis of a multilayer model of Leuning et al. (1995). The model was further refined by Wang (2000) and tested against eddy flux measurements in 14 different ecosystems (Wang et al., 2006).

The main features of CABLE are:

(1) a coupled model of stomatal conductance, photosynthesis and partitioning of absorbed net radiation into latent and sensible heat fluxes;
(2) the model differentiates between sunlit and shaded leaves, i.e. two-big-leaf submodel for calculation of photosynthesis, stomatal conductance, leaf temperature;
(3) radiation submodel calculates the absorption of beam and diffuse radiation in visible and near infrared wavebands, and thermal radiation;
(4) aerodynamic conductance for two big leaves is calculated using far field and near field theory for canopy turbulence (Raupach et al., 1997);
(5) a multilayer soil model is used; Richards equations are solved for soil moisture and heat conduction equation for soil temperature;
(6) snow model computes temperature, density and thickness of three snowpack layers.

CABLE computes photosynthesis (P_n), leaf (R_d), plant (autotrophic) (R_p) and soil (heterotrophic) (R_s) respiration. From these components, we calculate gross primary productivity as $GPP = P_n + R_d$, net primary productivity as $NPP = P_n - R_p$ and net ecosystem production as $NEP = P_n - R_p - R_s$. The flux of CO_2 to the atmosphere is $-NEP$, which we denote here as net ecosystem exchange (*NEE*), i.e. $NEE = -NEP$. (Recall that fluxes from land-use change are not calculated by CABLE and are run as a separate tracer in this simulation.)

A simple carbon pool model based on Dickinson et al. (1998) is used to describe the allocation of photosynthesis product and the flow of carbon between the vegetation carbon and soil pools. The wood and roots carbon pools are used to calculate the wood and root respiration fluxes, however the leaf carbon pool is not used to determine leaf area index (LAI), which is prescribed using monthly MODIS data (Myneni et al., 2002). We used the MOD15_BU $0.25 \times 0.25^\circ$ product, averaging (by month) all the available months (April 2000 to September 2003) at the time the model run was set up (ftp://primavera.bu.edu/pub/datasets/MODIS/). Note that this neglects interannual variations in LAI. Carbon flow from plant to soil pool is calculated from the prescribed seasonal LAI for leaves and, for woody tissue and roots, it is assumed to be proportional to the amount of plant biomass carbon.

In this experiment, CCAM has a horizontal resolution of 200 km. The model time step of 30 min is the same for CCAM and CABLE, allowing the models to be synchronously coupled (although here the simulation required prescribed CO_2 forcing). We used 11 vegetation types and 9 soil types with all biophysical properties described in look–up tables. Only three key model parameters were estimated for each vegetation type: maximum carboxylation rate ($v_{\mathrm{cmax},25}$), plant respiration rate (r_p) and soil respiration rate (r_s) at optimal soil water level at 25°C. The parameters were estimated by running the model under present-day conditions. Firstly, GPP was calculated for each vegetation type for six values of $v_{\mathrm{cmax},25}$ ranging from 10 to 250 μmol m^{-2}s^{-1} and keeping all other model parameters constant. From this, $v_{\mathrm{cmax},25}$ was estimated by assuming $GPP = 2 \times NPP$ and using NPP estimates from the CASA model. As a second step, r_p and r_s were tuned to give plant respiration and soil respiration equal to NPP. The tuning method is described in more detail in Wang and Barrett (2003).

3.3. Spin-up

Two steps were performed for the purpose of carbon pool initialization; one for the calculation of the atmospheric forcing and soil variables, and the other for actual initialization. In the first step, the fully coupled model was forced with prescribed SSTs; at each time step and for each grid-cell the values of all the atmospheric forcing variables and soil/snow prognostic variables were saved for 1 yr. In the second step, CABLE was run using the atmospheric forcing and soil/snow variables from the first step. In response, CABLE calculated carbon uptake and loss by plants, allocation of carbon between leaf, root and wood pools, and soil carbon. The initial global total pool sizes were taken from CASA (leaf 21.2 PgC, wood 542.0 PgC, roots 64.9 PgC and soil 510 PgC). The model was run several times for 1900 using the prescribed forcing scenario, assumed rates of decomposition and transfer. The transfer rates between pools were tuned until the carbon pools came approximately to equilibrium at values close to the CASA totals. The predicted pool sizes were leaf 30.2 PgC, wood 520 PgC, roots 62.7 PgC and soil 580 PgC.

4. Comparison with atmospheric CO_2

Coupled carbon-climate simulations are computationally expensive and generate large amounts of model data. How to best validate that data is an open question and one that deserves investigation. Here, we focus the analysis of the model simulation on atmospheric CO_2 for a number of reasons. Firstly, atmospheric mixing means that observed CO_2 concentrations integrate fluxes over a region. Thus, comparisons can be made more reliably than those that directly compare fluxes for a grid-cell with, for example, flux tower measurements. Secondly, one of the goals of carbon-climate work is to determine whether CO_2 will accumulate in the atmosphere more or less quickly when carbon feedbacks are accounted for. Thus, it is vital that we check whether we are able to adequately simulate the last two decades of atmospheric CO_2. Thirdly, different elements of the atmospheric measurements can highlight different capabilities of the modelled biosphere fluxes. For example, the ability to model changes in global growth rate can comment on the biosphere response to interannual climate variability while spatial gradients of CO_2 can highlight problems with the global distribution of annual mean NEE.

4.1. Global growth rate

While biosphere carbon was modelled for the whole of the 20th century, the other contributions to atmospheric CO_2 i.e. fossil, ocean and land-use fluxes were only modelled from 1960. We compare modelled and observed CO_2 concentration from this time at Mauna Loa, Hawaii (Keeling and Whorf, 2005). The global mean modelled concentration at the start of 1960 was set to 316.35 ppm which was taken from the CO_2 forcing provided for the experiment. Modelled and observed CO_2 are therefore close in magnitude during the early 1960s. During the next two decades, modelled CO_2 increases more rapidly than the observations, while in the 1980s and 1990s, the growth rates are similar (Fig. 1). The growth rates were calculated by taking the difference in annual mean CO_2 concentration from one year to the next. In addition to the decadal changes in growth rate, there are also interannual variations due to the influence of climate on carbon fluxes. We will discuss these in Section 4.2.

Decadal carbon budgets are given in Table 1. The atmospheric increase is taken from the Mauna Loa record and converted to PgC yr^{-1} using a factor of 2.123 PgC ppm^{-1} while the other fluxes are global integrals. The modelled atmospheric increase is around 1 PgC yr^{-1} too large in the 1960s and 1970s, but only around 0.3 PgC yr^{-1} too large in the 1980s and 1990s. It is not possible to categorically attribute this error to the biosphere simulation, but it is probable that the modelled NEP is too small. For example, the four terrestrial models used in McGuire et al. (2001) gave NEE of −1.1 to −2.3 PgC yr^{-1} in the 1980s compared to −0.5 PgC yr^{-1} here.

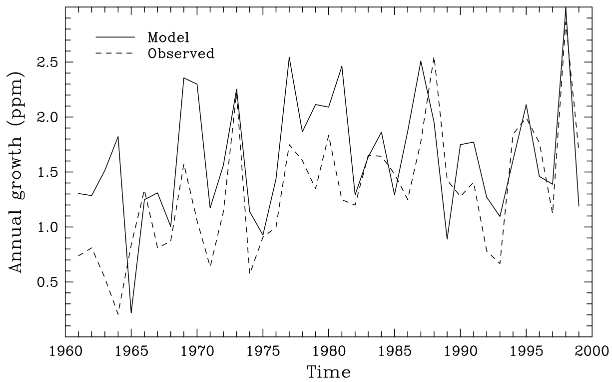

Fig. 1. Modelled (solid) and observed (dashed) annual growth in CO_2 concentration at Mauna Loa (19.5°N, 155.6°W).

Table 1. Carbon fluxes for the decades 1960 – 1969, 1970 – 1979, 1980 – 1989 and 1990 – 1999 in PgC yr^{-1}. The atmospheric increase is calculated using Mauna Loa data and will only approximate the global atmospheric increase and closure of the budget

Flux	1960s	1970s	1980s	1990s
Atm inc MLO (obs)	1.83	2.75	3.32	3.05
Atm inc MLO (mod)	2.96	3.69	3.63	3.33
Prescribed fossil	3.12	4.75	5.52	6.36
Prescribed ocean	−1.25	−1.64	−2.06	−2.43
Prescribed land-use	1.16	1.15	0.80	0.74
Modelled NEE	−0.14	−0.67	−0.47	−1.17

Comparing our budgets with those reported in Prentice et al. (2001), we lie within the uncertainty ranges for the 1980s, but in the 1990s the ocean uptake we have prescribed is too large and the modelled land uptake is too small. In the 1980s, our results are near the lower end of the land-use contribution and the upper end of the residual terrestrial sink. It is possible that processes that are currently neglected by CABLE, such as nitrogen fertilisation, could increase the terrestrial sink. The difference in NEE from the 1980s to the 1990s is around half the difference given in the Prentice et al. (2001) budget if we assume that the contribution from land-use is similar between decades.

The contributions to NEE are shown in Fig. 2. GPP, NPP and soil respiration (R_s) increase over the century, consistent with increasing CO_2 and temperature. The magnitude of the fluxes appears slightly large compared to other estimates. Our modelled GPP ranges from about 118–132 PgC yr^{-1} compared to the MODIS based estimate of 109 PgC yr^{-1} for 2001 – 2003 (Zhao et al., 2005). The average NPP for 1980 – 1999 is 70 PgC yr^{-1}. This is around 12–16% larger than the values quoted

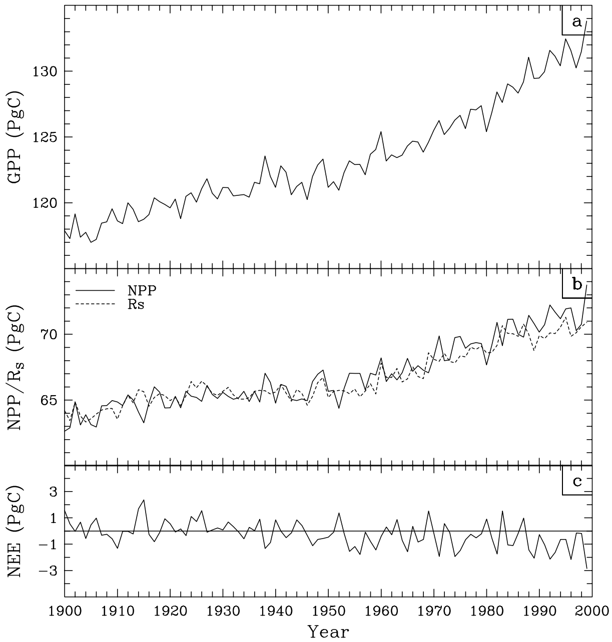

Fig. 2. Global GPP (a), NPP and R_s (b) and NEE (c).

for NPP in the 2001 IPCC report (59.9 and 62.6 PgC yr^{-1}, Prentice et al., 2001). The CABLE NPP is also at the top end of the NPP range produced by a number of models that participated in the Potsdam intercomparison (44–66 PgC yr^{-1} excluding two outliers, Cramer et al., 1999). Comparing with the latitudinal distribution shown in Fig. 1 of Kicklighter et al. (1999), our results are close to the median in the northern mid and high latitudes but at the top of the range around 15°N and 10–30°S.

NEE, plotted in Fig. 2 with positive indicating a source of CO_2 to the atmosphere, is the small difference between large photosynthesis and respiration fluxes. We have assumed a near neutral biosphere at the start of the century and tuned the model to achieve this. The modelled NEE is unconstrained from this point (except through the feedback between carbon pool size and respiration) and becomes a small sink by the end of the century.

4.2. *Interannual variability*

Figure 1 shows year-to-year changes in the growth rate at Mauna Loa of up to 1 ppm yr^{-1} for both modelled and observed CO_2. The variations are reasonably similar with a correlation of 0.60. The observed CO_2 growth rate is known to vary with El Niño-Southern Oscillation (ENSO) events; changes in ocean circulation alter the air–sea exchange of CO_2 and changes in temperature and precipitation impact on biosphere exchange and fire events. The emissions from fire are thought to make a major contribution to the anomaly (Langenfelds et al., 2002). Since we model the atmospheric concentration from anthropogenic, ocean and biosphere fluxes separately, we have calculated Mauna Loa growth rates for each tracer to determine which dominates the modelled interannual variability (IAV). Note however that interannual variations from the ocean fluxes will be minimal since the ocean simulations from which the fluxes were taken included no interannual forcing. The CABLE NEE tracer produces the largest variations in growth rate (comparable in magnitude to the variations from the summed tracers) with a correlation of 0.94 between the detrended NEE-only growth-rate and the detrended growth-rate from all modelled fluxes. Clearly, in our simulation, the IAV is dominated by interannual variations in NEE. The NEE variations are largest for the two tropical vegetation types (broadleaf evergreen and savanna) and both correlate with global NEE at greater than 0.7. Given that we are matching the magnitude of the anomalies from changes in NEE alone without contributions from fire, this implies that modelled NEE may be unduly sensitive to climate variation.

We compare the interannual variations in CO_2 fluxes and climate variables over the 20th century by first removing decadal and longer variations from the timeseries. We fit a smoothing spline with 50% attenuation at 20 yr (Enting, 1987) and remove this from the timeseries. The interannual variations in global NEE correlate more strongly with those in NPP (−0.82) than with those in soil respiration (0.51). The variations in NEE are mostly larger than those in NPP or R_s. Interannual variability in NEE shows a moderate correlation (0.58) with IAV in global land temperature. Interestingly the correlation with temperature for both NPP and R_s is weaker than for NEE. ENSO contributes to IAV in global temperature and so we also find moderate correlation between NEE and the Southern Oscillation Index (−0.45). The correlation with the SOI is similar if we consider only the period of the Mauna Loa record (1960 – 1999) but increases to −0.63 if we neglect years that may be affected by large volcanic eruptions (1962 – 1963 for Agung, 1982 – 1983 for El Chichon and 1991 – 1992 for Pinatubo). Volcanoes are expected to impact on global NEE not only through cooling of the atmosphere but possibly also by changes in direct and diffuse radiation. The correlation of IAV in precipitation with IAV in NEE (−0.27) is much weaker than with temperature and also of opposite sign. This is expected since drier conditions will tend to decrease photosynthesis and increase respiration and result in a decreased sink or increased source of CO_2 to the atmosphere.

4.3. *Annual mean distribution*

The spatial distribution of CO_2 provides useful information about the spatial distribution of surface fluxes. It is possible to model reasonable global fluxes but have compensating errors; the annual mean distribution of atmospheric CO_2 provides a very sensitive test for our modelled fluxes because it responds to the annual net CO_2 flux which is the small difference of large seasonal fluxes. Figure 3 shows the mean modelled concentration for 1980 – 1999 at 84 sites compared to observations. Both sets of data are plotted relative to the South Pole concentration to facilitate a direct comparison. The observed values are taken

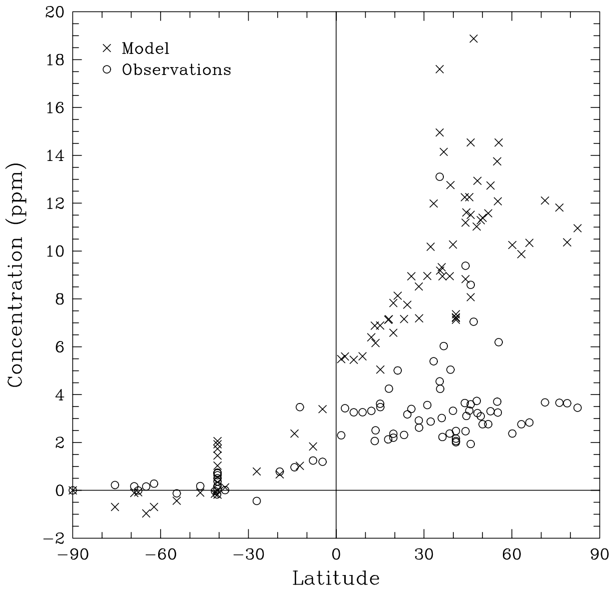

Fig. 3. Modelled (x) and observed (o) mean CO_2 concentration for 1980 – 1999 at 84 sampling locations relative to the mean concentration at the South Pole. The observations are from GLOBALVIEW-CO_2 (2003) and include gap-filled data.

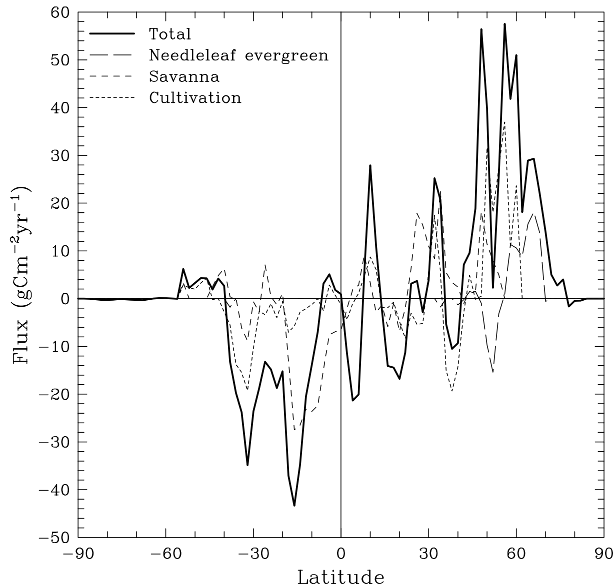

Fig. 4. Zonal mean total NEE and the contribution from three vegetation types listed in the key

from GLOBALVIEW-CO_2 (2003). This is a data product that provides pseudo-weekly CO_2 for each site by fitting the CO_2 flask or in-situ observations with a smooth curve (Masarie and Tans, 1995). A data extension technique provides the option of filling gaps in the records. Here, we use the extended data to give maximum spatial coverage over the last two decades.

The model gives a much larger north–south gradient in concentration than is seen in the observations. This implies either a major problem with interhemispheric mixing in the model or that northern hemisphere fluxes are too large compared to southern hemisphere ones. It is unlikely that the problem is with model transport since the interhemispheric difference in CO_2 from the fossil emissions alone is 4.5 ppm, which is in the middle of the range produced by other models (3.5–5.3 ppm, adjusted to account for a small difference in total fossil emissions) (Gurney et al., 2003). Since the ocean and land-use fluxes make little contribution to the north–south gradient of CO_2, the incorrect gradient indicates problems with the distribution of NEE fluxes and/or missing fluxes due to processes that are not modelled here.

The annual zonal mean NEE flux for 1980 – 1999 is shown in Fig. 4. It shows a sink in the southern low-mid latitudes and a source in the northern mid-high latitudes, consistent with the overestimate found in the north–south gradient of atmospheric concentration. Also shown in Fig. 4 is the contribution from three of the vegetation types. The two main contributors to the southern sink are cultivation and savanna. Cultivation also contributes to the northern source along with needleleaf evergreen, other forests and tundra (not shown). The relatively large net fluxes produced by the cultivation biome are almost certainly unrealistic; the shorter lifetime of crops and pasture compared to trees would suggest that the cultivation biome should be near to neutral over the annual cycle. Goodale et al. (2002) find a temperate northern forest sink of around 0.6 PgC yr^{-1} which we do not see in our model results. However, at least some of the difference is likely due to processes that we do not model, such as fire suppression, recovery from disturbance and woody encroachment. Tropical deforestation, which we also neglect here, would likely offset some of the modelled southern low-latitude sink.

4.4. Seasonal cycles

The seasonal cycle of atmospheric CO_2 is dominated by the seasonal exchange of CO_2 with the biosphere, particularly in the northern hemisphere. We have calculated average (1980 – 1999) seasonal cycles for each site by fitting a smoothing spline with 50% attenuation at 3 yr (Enting, 1987) to the monthly time-series of concentration, subtracting this smooth curve from the monthly concentrations and averaging the remaining concentrations by month of the year. We compare these seasonal cycles to those provided for 1979 – 2001 in the GLOBALVIEW-CO_2 (2003) product. Figure 5a shows the peak-to-peak amplitude (the difference between minimum and maximum monthly concentration) for each site while Fig. 5b shows the month of the minimum concentration as an indicator of the phase of the seasonal cycle. Overall the amplitude is well modelled in the southern hemisphere and the high northern latitudes. From 10–50°N, the model tends to underestimate the amplitude. The underestimate is widespread including both continental and marine sites.

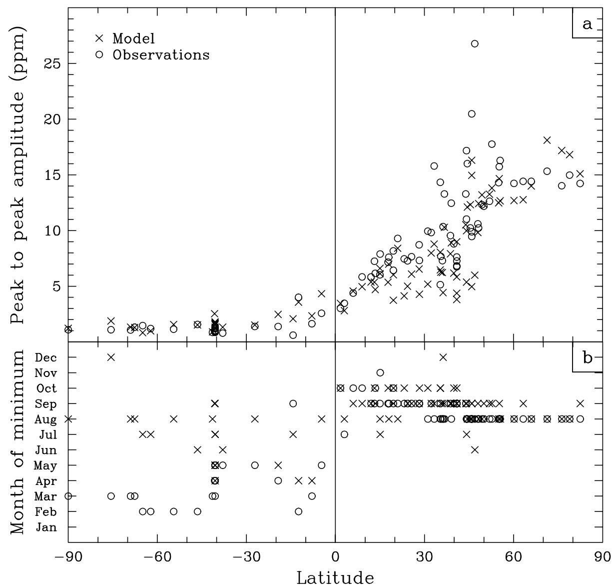

Fig. 5. Peak-to- peak amplitude of the seasonal cycle (a) at observing sites and the month of the minimum concentration (b) for the model (x) and observations (o).

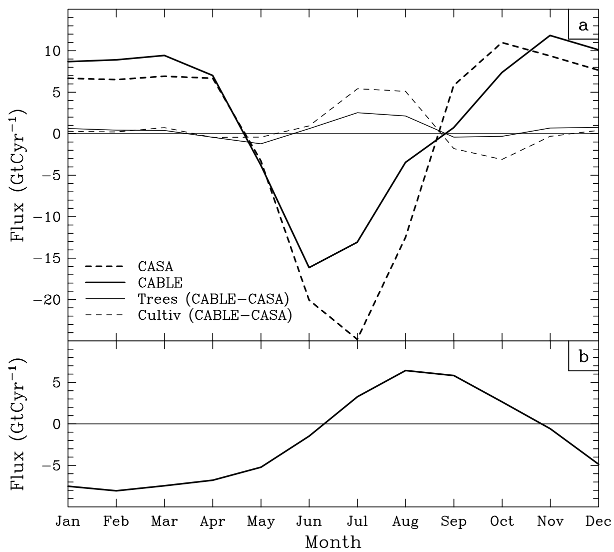

Fig. 6. NEE fluxes from CABLE (bold, solid) and CASA (bold, dashed) for 30–90°N (a) and from CABLE (bold, solid) for 0–30°S (b). Also shown in panel (a) are the differences in flux between CABLE and CASA for two vegetation types, broadleaf and needleleaf trees (solid) and cultivation (dashed).

Figure 6a shows the CABLE NEE fluxes for 30–90°N. For comparison, CASA fluxes are also shown. The uptake produced by CABLE is smaller than CASA from June to August, indicating that reduced summer uptake is the cause of the underestimate in modelled atmospheric CO_2 amplitude. For July and August, the difference is principally in the 30–60°N region and in the 'broadleaf and needleleaf trees' and 'cultivation' vegetation types. It is difficult to determine whether the problem is with too little photosynthesis or too much respiration, but given that the simulated NPP by CABLE is quite high compared to other models this would suggest the problem is with soil respiration. We suspect that the soil respiration may be too sensitive to soil temperature.

It seems unlikely that problems with the atmosphere model climate are to blame since the reduced uptake is widespread in space and occurs over most of the summer season. To confirm this, we reran the last 7 yr of the simulation nudging the atmospheric model to NCEP analysed winds and temperature (Kalnay et al., 1996; Collier, 2004), thereby removing any climate biases from our atmospheric simulation. NCEP sea surface temperatures were also used. Analysis of the 1995 – 1999 results showed no significant improvement in the modelled seasonal amplitude. Many northern hemisphere sites showing a slightly poorer agreement with observations in winter and little change to the minimum concentration in summer.

The phase of the seasonal cycle (Fig. 5b) is good in the northern hemisphere, with the model sometimes leading the observations by a month. In the southern hemisphere, the model is mostly out of phase with the observations, sometimes by five or six months. It is not clear how much of the southern hemisphere seasonality is local and how much is transported from the northern hemisphere. To better understand this, we averaged the NEE fluxes for 1980 – 1999 and ran the model for 3 yr (1996 – 1998) prescribing these fluxes in each semi-hemisphere separately. For the South Pole (typical of other southern sites), we found the northern hemisphere contributions are in phase with the observed seasonal cycle while the 0–30°S contribution is not. Thus the implication of the incorrectly modelled phase would be that the flux seasonality is too small in northern latitudes (as we have already discussed) and too large in the southern tropics. Nemry et al. (1999) also found that the seasonal cycle at southern hemisphere sites was difficult to model correctly and was dominated by the contribution from NEE in the low southern latitudes.

The seasonality of NEE from CABLE for 0–30°S is shown in Fig. 6b. Two factors appear to contribute to the overestimated seasonality in this region; deficiencies in modelled climate and insufficient variability in modelled fluxes across the region. Firstly, in the short test run which removed climate simulation bias by using NCEP atmospheric forcing, the seasonality of the resulting CABLE fluxes from this region is reduced. Less source is simulated in the second half of the year while the fluxes in the first months of the year change little. However, the reduced flux seasonality only gives a slight improvement to the phasing of the atmospheric seasonal cycle of CO_2 in the southern hemisphere.

Secondly, there is observational evidence that the seasonal cycle may be more variable across this tropical region than is found by CABLE. We find wet season uptake and dry season release to the atmosphere at five sample locations across Brazil. However for at least one of these locations, Tapajos, flux tower results give a source from January to August and sink from September to December (Saleska et al., 2003), opposite to the modelled fluxes. This appears to be a common model problem because Saleska et al. (2003) show that two other terrestrial models also give opposite seasonality to the observations. Saleska et al. (2003) found that respiration responded strongly to seasonal variations in precipitation with 40% greater respiration in March (wet season) than November (dry season). By contrast, photosynthesis only responded weakly to precipitation because the trees are able to access deep soil water during dry periods. Thus, respiration dominated the seasonality of the net flux. Using CABLE, the respiration fluxes at Tapajos are almost constant throughout the year and the net flux is dominated by seasonality in photosynthesis. While we have some moisture dependence in our soil respiration calculation, it is clearly too weak in this region. Our model response to precipitation in the tropics requires further work along with improving our climate simulation for this region.

4.5. Diurnal cycles

The diurnal cycle of atmospheric CO_2 at any given location is dependent on both the diurnal cycle of fluxes in the immediate vicinity and the diurnal cycle in mixing. Observations from tower sites typically show well-mixed conditions during the afternoon but large vertical gradients of CO_2 at night when shallow boundary layers can occur. Figure 7 shows the peak-to-peak amplitude of the observed median diurnal cycle provided in GLOBALVIEW-CO_2 (2003) at three tower sites: LEF (45.9°N, 90.3°W), ITN (35.4°N, 77.4°W) and HUN (47.0°N, 16.7°E). In each case, the amplitude increases in summer when the diurnal amplitude of the fluxes increases. Also shown in Fig. 7 are the modelled mean diurnal amplitudes. These follow a similar pattern to the observations, although the summer increase tends to occur too early and decrease too late. In mid-summer at LEF, the modelled amplitude in the surface layer (mid-point approximately 40 m) is similar to the observed amplitude at 11 m and larger than the amplitude at 30 m. Assuming modelled vertical mixing is reasonable, this implies that the diurnal amplitude of modelled fluxes is too large. At ITN, the modelled diurnal amplitudes appear to be too small in summer and too large in winter, while at HUN the modelled amplitudes show reasonable agreement with the observations.

At LEF, the overestimated amplitude in winter most likely implies an overestimate in respiration since little photosynthesis occurs during winter. In summer, both respiration and photosynthesis may be too large with any overestimate in respiration being amplified by the shallow night-time boundary layer. These features are seen in Fig. 8 which compares the modelled fluxes with flux measurements from LEF (Davis et al., 2003; Falge et al., 2005). While we should not expect perfect agreement between model grid-cell average fluxes and those calculated at a tall tower, the gross differences shown in Fig. 8 do support the assertion of overestimated fluxes deduced from the diurnal amplitude of atmospheric CO_2. In particular, the night-time (respiration) fluxes from the model are about twice those observed. This is a significant problem given that the observed respiration fluxes are large compared to those from other flux towers in the area (Desai et al., 2006). Day-time fluxes are also overestimated except in the middle of summer. This implies that photosynthesis is too large early and late in the growing season. The total flux in mid-summer is a source in the model compared to a sink in the observations which is consistent with the underestimated seasonal cycle at this latitude shown in Fig. 5.

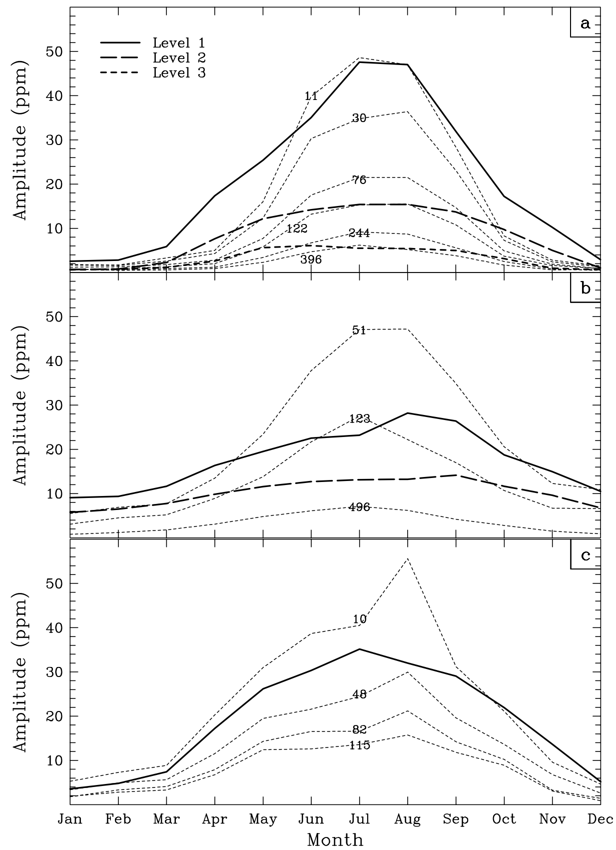

Fig. 7. Peak-to- peak amplitude of the mean modelled diurnal cycle (bold lines) and median observed diurnal cycle (dotted lines) of atmospheric CO_2 concentration in each month for LEF (a), ITN (b) and HUN (c). The observed lines are labelled with the sampling height in metres. The model vertical coordinate is sigma (pressure/surface pressure) with mid-model levels of 0.996, 0.978 and 0.946 for the lowest three levels, corresponding to approximate heights above the surface of 37, 179 and 456 m. Model output was not available for all levels at all three locations.

5. Discussion and conclusions

Comparison of modelled and observed atmospheric CO_2 has highlighted a number of deficiencies with our simulation of

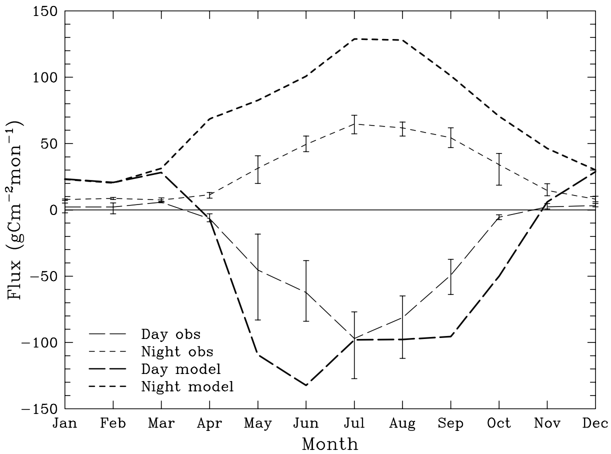

Fig. 8. Day and night NEE flux for the model grid-cell containing LEF (bold) and flux tower observations (standard). The model fluxes are averaged over 1980 – 1999. The flux tower observations are averaged over 1997 – 1999. The error bars span the minimum and maximum value from any of the three years.

biosphere carbon fluxes. Global GPP and NPP are both slightly larger than we expect while NEP is too small (i.e. not enough carbon uptake) particularly in the northern hemisphere. The GPP and NPP may be improved if our modelling of photosynthesis included some simple phenology rules to capture the onset and cessation of photosynthesis. Currently, the onset of photosynthesis uses a temperature threshold which does not appear to work well for all parts of the globe. For example, at high altitude in central Asia the threshold is never met and no photosynthesis occurs. We also need to include interactive LAI as our current use of prescribed values does not allow for any interannual variability and consequently the response of the biosphere to climate variability may be oversimplified.

The problems that we have found with NEE are largely due to an overestimation of respiration. Currently, respiration in CABLE is mainly driven by temperature. This temperature sensitivity appears to be too strong and the problem is enhanced by a warm temperature bias in the northern hemisphere in our current simulation. We need to implement more realistic plant and soil respiration models with dependence on a number of variables. In the tropics, the seasonality of soil respiration was found to be dependent on soil moisture, and while this is currently included in our model the temperature response dominates.

Our simulation for 1980 – 1999 allocates to the savanna biome about 25% of global GPP (which is reasonable) and about 50% of NPP (which seems to be too large). Savanna is largely occupied by C4 grassland, so this implies that our treatment of C4 plants in the model may need to be refined, with an increase in plant respiration required.

In addition to the model development required to correct the more substantive problems with our simulation, we also need to extend the capability of CABLE to include land-use change and the impact of anthropogenic nitrogen addition on carbon fluxes. The ability to model dynamic vegetation will also be important for simulations out to 2100. Inclusion of carbon isotopes and carbonyl sulfide (COS) would provide useful diagnostics of modelled photosynthesis and respiration.

We have taken a step towards a fully coupled run for the 21st century by repeating the final 40 yr of the current simulation with the biosphere seeing the modelled CO_2 concentration rather than the prescribed forcing. Preliminary results show greater CO_2 uptake by the biosphere in the 1980s and 1990s but little or no improvement in the modelled seasonal cycles and annual mean north–south gradient.

The large range of results coming out of current carbon-climate simulations of the 21st century (Friedlingstein et al., 2006) means that it is vital to evaluate the component models as thoroughly as possible. We have demonstrated here that atmospheric CO_2 concentrations on a range of time-scales can make an important contribution to the necessary evaluation; long-term trends, interannual variability, seasonal and diurnal cycles target a variety of flux behaviour in time while concentration gradients highlight information about the spatial distribution of fluxes. While a good simulation of the past century does not guarantee correct model behaviour into the future, we may want to give more weight to the results of those models that do achieve a credible simulation of current conditions.

6. Acknowledgements

We thank the Australian Greenhouse Office for support of this work, John McGregor for providing CCAM and Bernard Pak and Peter Rayner for helpful comments on the manuscript. This type of study could not happen without the contributions of atmospheric CO_2 data by many people to the GLOBALVIEW-CO_2 compilation and the data processing work of Ken Masarie. Flux measurements and analyses at the WLEF tower were supported by the Office of Science (BER) U.S. Department of Energy via the Midwestern Regional Center of the National Institutes for Global Environmental Change under cooperative agreement number DE-FG03–90ER61010, and via the Terrestrial Carbon Processes program, grant number DE-FG02–03ER63681. Mixing ratio measurements were supported by the Atmospheric Chemistry Project of the Climate and Global Change Program of the National Oceanic and Atmospheric Administration.

References

Andres, R. J., Marland, G., Fung, I. and Matthews, E. 1996. A 1° ×1° distribution of carbon dioxide emissions from fossil fuel consumption and cement manufacture, 1950 – 1990. *Global Biogeochem. Cycles* **10**, 419–429.

Collier, M. A. 2004. The CSIRO NCEP/NCAR/DOE *R-1/R-2 archive*. *CSIRO Atmospheric Research technical paper* **68**, 75pp.

Cox, P. D., Betts, R. A., Jones, C. D., Spall, S. A. and Totterdell, I. J. 2000. Acceleration of global warming due to carbon-cycle feedbacks in a coupled climate model. *Nature* **408**, 184–187.

Cramer, W., Kicklighter, D. W., Bondeau, A., Moore, B. I., Churkina, G., and co-authors and the participants of the Potsdam NPP Model Intercomparison 1999. Comparing global models of terrestrial net primary productivity (NPP): overview and key results. *Glob. Change Biol.* **5** (Suppl. 1), 1–15.

Dargaville, R. J., Heimann, M., McGuire, A. D., Prentice, I. C., Kicklighter, D. W., and co-authors 2002. Evaluation of terrestrial carbon cycle models with atmospheric CO_2 measurements: results from transient simulations considering increasing CO_2, climate, and land-use effects. *Glob. Biogeochem. Cyc.* **16**, 1092. DOI=10.1029/2001GB001426.

Davis, K. J., Bakwin, P. S., Yi, C., Berger, B. W., Zhao, C. and co-authors, 2003. The annual cycles of CO_2 and H_2O exchange over a northern mixed forest as observed from a very tall tower. *Glob. Change Biol.* **9**, 1278–1293.

Desai, A. R., Noormets, A., Bolstad, P. V., Chen, J., Cook, B. D. and co-authors, 2006. Influence of vegetation and seasonal forcing on carbon dioxide fluxes across the Upper Midwest, USA: implications for regional scaling. *Agric. Forest Meteor.* (in press).

Dickinson, R. E., Shaikh, M., Bryant, R. and Graumlich, L. 1998. Interactive canopies for a climate model. *J. Climate* **11**, 2823–2836.

Dufresne, J. L., Friedlingstein, P., Berthelot, M., Bopp, L., Ciais, P. and co-authors, 2002. On the magnitude of positive feedback between future climate change and the carbon cycle. *Geophys. Res. Lett.* **29**, DOI:10.1029/2001GL013777.

Enting, I. G. 1987. On the use of smoothing splines to filter CO_2 data. *J. Geophys. Res.* **92D**, 10 977–10 984.

Etheridge, D. M., Steele, L. P., Langenfelds, R. L., Francey, R. J., Barnola, J. M. and co-authors. 1996. Natural and anthropogenic changes in atmospheric CO_2 over the last 1000 years from air in Antarctic ice and firn. *J. Geophys. Res.* **101D**, 4115–4128.

Falge, E., Aubinet, M., Bakwin, P., Berbigier, P., Bernhofer, C. and co-authors. 2005. FLUXNET Marconi Conference Gap-Filled Flux and Meteorology Data, 1992–2000. Data set. Available on-line [http//www. daac.ornl.gov] from Oak Ridge National Laboratory Distributed Active Archive Center, Oak Ridge, Tennessee, U.S.A.

Friedlingstein, P., Bopp, L., Ciais, P., Dufresne, J. L., Fairhead, L. and co-authors. 2001. Positive feedback between future climate change and the carbon cycle. *Geophys. Res. Lett.* **28**, 1543–1546.

Friedlingstein, P., Cox, P., Betts, R., Bopp, L., von Bloch, W. and co-authors. 2006. Climate–carbon cycle feedback analysis, results from the C^4MIP model intercomparison. *J. Climate*. **19**, 3337–3353.

GLOBALVIEW-CO_2. 2003. Cooperative Atmospheric Data Integration Project - Carbon Dioxide. CD-ROM, NOAA CMDL, Boulder, Colorado. [Also available on Internet via anonymous FTP to ftp.cmdl.noaa.gov, Path: ccg/co2/GLOBALVIEW].

Goodale, C. L., Apps, M. J., Birdsey, R. A., Field, C. B., Heath, L. S. and co-authors. 2002. Forest carbon sinks in the Northern Hemisphere. *Ecol. Appl.* **12**, 891–899.

Gurney, K. R., Law, R. M., Denning, A. S., Rayner, P. J., Baker, D. and co-authors. 2003. TransCom 3 CO_2 inversion intercomparison: 1. Annual mean control results and sensitivity to transport and prior flux information. *Tellus* **55B**, 555–579. doi:10.1034/j.1600–0560.2003.00049.x.

Heimann, M., Esser, G., Haxeltine, A., Kaduk, J., Kicklighter, D. and co-authors. 1998. Evaluation of terrestrial carbon cycle models through simulations of the seasonal cycle of atmospheric CO_2: first results of a model intercomparison study. *Glob. Biogeochem. Cyc.* **12**, 1–24.

Houghton, R. A. 2003. Revised estimates of the annual net flux of carbon to the atmosphere from changes in land use and land management 1850–2000. *Tellus* **55B**, 378–390.

Jones, C. and Warnier, M. 2004. Climate–land carbon cycle simulation of the 20th century: assessment of HadCM3LC C4MIP Phase 1 experiment. Technical Note 59 Hadley Centre, Meteorological Office, UK. http://www.metoffice.com/research/hadleycentre/pubs/HCTN/HCTN_59.pdf.

Kalnay, E., Kanamitsu, M., Kistler, R., Collins, W., Deaven, D. and co-authors. 1996. The NCEP/NCAR 40-Year Reanalysis Project. *Bull. Amer. Meteor. Soc.* **3**, 437–471.

Keeling, C. D. and Whorf, T. P. 2005. Atmospheric CO_2 records from sites in the SIO air sampling network. In: *Trends: A Compendium of Data on Global Change*, Carbon Dioxide Information Analysis Center, Oak Ridge National Laboratory, U.S. Department of Energy, Oak Ridge, Tenn., U.S.A.

Kicklighter, D. W., Bondeau, A., Schloss, A. L., Kaduk, J., McGuire, A. D. and the participants of the Potsdam NPP Model Intercomparison 1999. Comparing global models of terrestrial net primary productivity (NPP): global pattern and differentiation by major biomes. *Glob. Change Biol.* **5 (Suppl. 1)**, 16–24.

Langenfelds, R. L., Francey, R. J., Pak, B. C., Steele, L. P., Lloyd, J. and co-authors. 2002. Interannual growth rate variations of atmospheric CO_2 and its isotope δ^{13}C, H_2, CH_4 and CO between 1992 and 1999 linked to biomass burning. *Global Biogeochem. Cycles* **16**, 1048. doi:10.1029/2001GB001466.

Leuning, R., Kelliher, F. M., Pury, D. G. D. and Schulze, E. D. 1995. Leaf nitrogen, photosynthesis, conductance and transpiration: scaling from leaves to canopies. *Plant Cell Environ.* **18**, 1183–1200.

Marland, G., Boden, T. A. and Andres, R. J. 2005. Global, Regional, and National Fossil Fuel CO_2-Emissions. In: *Trends: A Compendium of Data on Global Change*, Carbon Dioxide Information Analysis Center, Oak Ridge National Laboratory, U.S. Department of Energy, Oak Ridge, Tenn., U.S.A.

Masarie, K. A. and Tans, P. P. 1995. Extension and integration of atmospheric carbon dioxide data into a globally consistent measurement record. *J. Geophys. Res.* **100**, 11 593–11 610.

Matthews, H. D., Weaver, A. J. and Meissner, K. J. 2005. Terrestrial carbon cycle dynamics under recent and future climate change. *J. Climate* **18**, 1609–1628. doi: 10.1175/JCLI3359.1.

McGregor, J. L. and Dix, M. R. 2001. The CSIRO conformal-cubic atmospheric GCM. *IUTAM Symposium on Advances in Mathematical Modelling of Atmosphere and Ocean Dynamics*. Kluwer, 197–202.

McGregor, J. L. 1987. Accuracy and initialization of a two-time-level split semi-Lagrangian model. Collection of papers presented at WMO/IUGG NWP symposium, Tokyo, 4–8 August 1987, 233–246.

McGregor, J. L. 1993. Economical determination of departure points for semi-Lagrangian models. *Mon. Wea. Rev.* **121**, 221–230.

McGregor, J. L. 1996. Semi-Lagrangian advection on conformal-cubic grids. *Mon. Wea. Rev.* **124**, 1311–1322.

McGuire, A. D., Sitch, S., Clein, J., Dargaville, R., Esser, G. and co-authors. 2001. Carbon balance of the terrestrial biosphere in the twentieth century: analyses of CO_2, climate and land use effects with four process-based ecosystem models. *Global Biogeochem. Cyc.* **15**, 183–206.

Myneni, R. B., Hoffman, S., Knyazikhin, Y., Privette, J. L., Glassy, J. and co-authors. 2002. Global products of vegetation leaf area and fraction absorbed PAR from year one of MODIS data. *Remote Sens. Environ.* **83**, 214–231.

Nemry, B., François, L., Gêrard, J. C., Heimann, M. and the participants of the Potsdam NPP Model Intercomparison 1999. Comparing global models of terrestrial net primary productivity (NPP): analysis of the seasonal atmospheric CO_2 signal. *Glob. Change Biol.* **5 (Suppl. 1)**, 65–76.

Prentice, I. C., Farquhar, G., Fasham, M., Goulden, M., Heimann, M. and co-authors. 2001. The carbon cycle and atmospheric carbon dioxide. In: *Climate Change 2001: The Scientific Basis. Contribution of Working Group I to the Third Assessment Report of the Intergovernmental Panel on Climate Change*, (eds.J. Houghton, Y. Ding, D. J. Griggs, M. Noguer, P. J. van der Linden, X. Dai, K. Maskell and C. A. Johnson), Cambridge University Press, Cambridge, United Kingdom and New York, NY, USA, 183–238.

Randerson, J. T., Thompson, M. V., Conway, T. J., Fung, I. Y. and Field, C. B. 1997. The contribution of terrestrial sources and sinks to trends in the seasonal cycle of atmospheric carbon dioxide. *Global Biogeochem. Cycles* **11**, 535–560.

Raupach, M. R., Finkele, K. and Zhang, L. 1997. SCAM (Soil-Canopy-Atmosphere Model): Description and comparison with field data. CSIRO Centre for Env. Mechanics Tech. Rep. 132.

Rayner, N. A., Parker, D. E., Horton, E. B., Folland, C. K., Alexander, L. V. and co-authors. 2003. Global analyses of sea surface temperature, sea ice, and night marine air temperature since the late nineteenth century. *J. Geophys. Res.* **108**, 4407. doi:10.1029/2002JD002670.

Saleska, S. R., Miller, S. D., Matross, D. M., Goulden, M. L., Wofsy, S. C. and co-authors. 2003. Carbon in Amazon forests: unexpected seasonal fluxes and disturbance-induced losses. *Science* **302**, 1554–1557.

Wang, Y. P. and Barrett, D. J. 2003. Estimating regional terrestrial carbon fluxes for the Australian continent using a multiple-constraint approach. I. Using remotely sensed data and ecological observations of net primary production. *Tellus* **55B**, 270–289. doi:10.1034/j.1600-0560.2003.00031.x.

Wang, Y. P. and Leuning, R. 1998. A two-leaf model for canopy conductance, photosynthesis and partitioning of available energy I. Model description and comparison with a multi-layered model. *Agric. Forest Meteor.* **91**, 89–111.

Wang, Y. P., Baldocchi, D., Leuning, R., Falge, E. and Vesala, T. 2006. Estimating parameters in a land surface model by applying nonlinear inversion to eddy covariance flux measurements from eight FLUXNET sites. *Glob. Change Biol.* (in press).

Wang, Y. P. 2000. A refinement to the two-leaf model for calculating canopy photosynthesis. *Agric. Forest Meteor.* **101**, 143–150.

Zeng, N., Qian, H., Munoz, E. and Iacono, R. 2004. How strong is carbon cycle-climate feedback under global warming? *Geophys. Res. Lett.* **31**, L20203. doi:10.1029/2004GL020904.

Zhao, M., Heinsch, F. A., Nemani, R. R. and Running, S. W. 2005. Improvements of the MODIS terrestrial gross and net primary production global data set. *Remote Sens. Environ.* **95**, 164–176.